Journal of Solid State Chemistry **154,** 435–443 (2000)
doi:10.1006/jssc.2000.8861, available online at http://www.idealibrary.com on IDEAL®

On the Existence of $Bi_{6.67}O_4(XO_4)_4$ and $PbBi_6O_4(XO_4)_4$ (X=P,V, and As)

Sophie Giraud,*,† Michel Drache,* Pierre Conflant,* Jean Pierre Wignacourt,*,[1] and Hugo Steinfink†

** Laboratoire de Cristallochimie et Physicochimie du Solide, UPRES A CNRS 8012, E.N.S.C.L., BP 108, 59652 Villeneuve d'Ascq Cedex, France; and † Texas Materials Institute, Department of Chemical Engineering, University of Texas, Austin, Texas, 78712*

Received February 17, 2000; in revised form June 15, 2000; accepted July 13, 2000; published online September 30, 2000

$PbBi_6O_4(PO_4)_4$ obtained at room temperature is isomorphous with the high-temperature phase $Bi_{6.67}O_4(PO_4)_4$. The Pb atom replaces 0.67 Bi in the same crystallographic site. The vanadate and arsenate with the composition $PbBi_6O_4(XO_4)_4$ were synthesized and yielded isomorphic phases at room temperature. All three compounds adopt a triclinic cell, space group $P\bar{1}$, Z=1. The structure refinement of $PbBi_6O_4(PO_4)_4$ was performed using the Rietveld method on X-ray powder diffraction data. The starting parameters were the atomic positions of $Bi_{6.67}O_4(PO_4)_4$. Conductivity measurements were made from 300°C to 800°C on samples of the three homologues. The highest conductivity was observed for the vanadate. Attempts to synthesize the binary vanadate and arsenate compounds isostructural with the high-temperature phase $Bi_{6.67}O_4(PO_4)_4$ were unsuccessful. © 2000 Academic Press

Key Words: **$Bi_{6.67}O_4(PO_4)_4$; $PbBi_6O_4(PO_4)_4$; isomorphism of $PbBi_6O_4(VO_4)_4$; $PbBi_6O_4(AsO_4)_4$.**

INTRODUCTION

The binary system Bi_2O_3–P_2O_5 has been previously investigated and it comprises many compounds (1–6). One such phase corresponds to the ratio $P/(Bi + P) = 0.389$ (3) and is reported as a high-temperature phase that appears at 910°C. The exact formula was recently determined as $Bi_{6.67}O_4(PO_4)_4$, $P/(Bi + P) = 0.375$, and the structure was solved by Ketatni *et al.* (1). They showed that the substitution of 0.67 Bi by a divalent cation $M = Sr^{2+}, Cd^{2+}, Ca^{2+}, Pb^{2+}$ to form $MBi_6P_4O_{20}$ or of 0.16 Bi by a monovalent cation $A = Li^+, Na^+, K^+$ to form $A_{0.5}Bi_{6.5}O_4(PO_4)_4$ stabilized the $Bi_{6.67}O_4(PO_4)_4$ phase at room temperature.

The study of the binary system Bi_2O_3–V_2O_5 (7, 8) and of substitutions in the $Bi_4V_2O_{11}$ (9) compound, generally labeled BIMEVOX, has been intensive because of the high ionic conductivity found in these compounds (10, 11). For that reason many phases in the pseudo ternary systems Bi_2O_3–MO–X_2O_5 (X = P, V, As and M = Pb, Ca, Ni, Mg, Sr, and others) have been investigated (12–21).

$PbBi_6O_4(PO_4)_4$ exists (1) and this paper reports the existence of the isomorphous vanadate and arsenate phases at room temperature. This finding also led us to reinvestigate the binary systems Bi_2O_3–X_2O_5 (X = V, As) to check for the existence of $Bi_{6.67}O_4(PO_4)_4$-type phases. The structural refinement of $PbBi_6O_4(PO_4)_4$ was carried out on powder X-ray diffraction data using the FULLPROF program (22) for the Rietveld refinement process.

EXPERIMENTAL

The syntheses of the phosphates and vanadates were carried out using Bi_2O_3 that was preheated at 600°C to remove any carbonates, PbO, and $(NH_4)_2HPO_4$ or V_2O_5. The phosphate with the stoichiometric composition was slowly heated to 300°C to decompose the diammonium hydrogen phosphate and the vanadate mixture was heated at 500°C. These compounds were held at these temperatures for about 10 hours. The temperatures were then raised to 800°C for 1 week with intermediate grinding to ensure that the reaction goes to completion.

The synthesis of the arsenates required extra precautions. In order to avoid any loss of arsenic, $BiAsO_4$ was used. It was obtained by mixing equimolar aqueous solutions of $Bi(NO_3)_3 \cdot 5H_2O$ and $NH_4H_2AsO_4$. For the ternary compounds, stoichiometric mixtures of $BiAsO_4$, Bi_2O_3, and PbO were slowly and carefully heated at 400°C, 550°C, and 750°C with intermediate grinding. The gold boats containing As were weighed each time to detect any loss of arsenic.

The single-phase purity of all synthesized products was confirmed by powder X-ray diffraction using a Guinier–De Wolff camera and Cu$K\alpha$ radiation. Differential thermal analysis (DTA) was performed on a Setaram instrument and high-temperature X-ray diffraction (HTXRD) on a Guinier–Lenné camera to determine whether any high-temperature phases for the vanadate and arsenate exist.

[1] To whom correspondence should be addressed. Telephone: (33) 320436542. Fax: (33) 320436814. E-mail: wignacourt@ensc-lille.fr.

0022-4596/00 $35.00

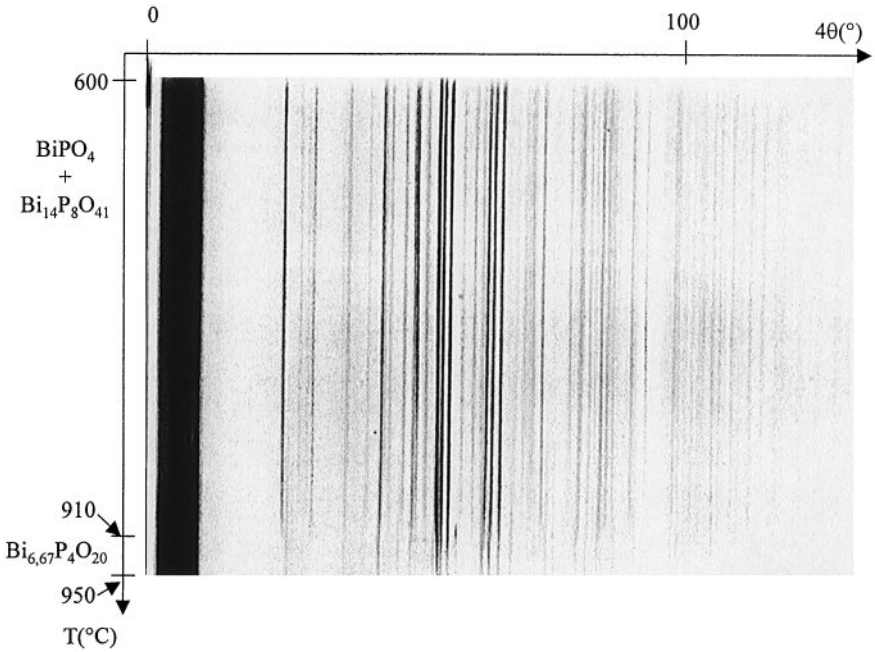

FIG. 1. High-temperature diffraction diagram (HTXRD) of $Bi_{6.67}O_4(PO_4)_4$.

Powder X-ray diffraction data used for structure refinement were recorded at room temperature on a Siemens D5000 $\theta/2\theta$ diffractometer, using a Bragg–Brentano geometry, with a diffracted beam monochromator and Cu$K\alpha$ radiation. The data collection and refinement parameters are shown in Table 3.

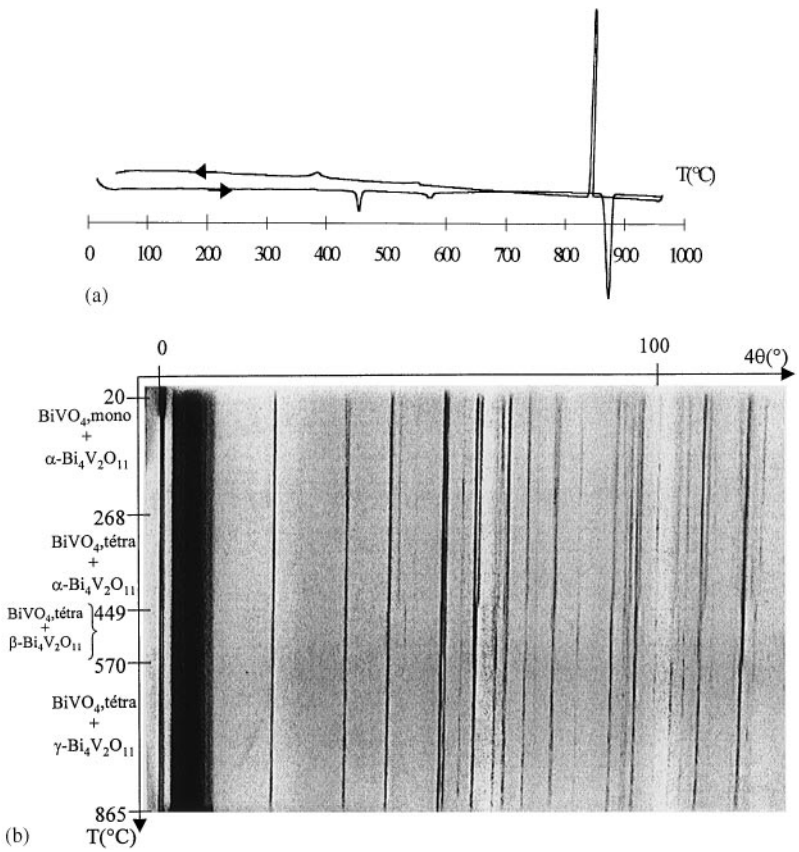

FIG. 2. Thermal analysis of the composition $Bi_{6.67}O_4(VO_4)_4$. (a) DTA; the arrows indicate the cooling and heating cycle. (b) HTXRD.

For conductivity measurements the powder samples were pelletized at room temperature and then sintered 50° below their meeting points for 2 hours. In every case compaction was in the 90 to 95% range. Gold electrodes were sputtered on both flat surfaces. Measurements were performed by impedance spectrometry in the frequency range $1–10^6$ Hz with a Schlumberger 1170 frequency response analyzer. At each temperature the measurement was made after the sample had equilibrated for at least 1 hour.

RESULTS

As mentioned $Bi_{6.67}O_4(PO_4)_4$ forms at 910°C (1) while at lower temperatures a mixture of $BiPO_4$ and $Bi_{14}P_8O_{41}$ (3) is observed (Fig. 1). DTA does not display any features that can be related to the appearance of any other phase.

The same analysis was performed on the $Bi_{6.67}O_4(VO_4)_4$ composition. The DTA displays three endothermic peaks at 455°C, 575°C, and 875°C, which can be attributed to the melting temperature (Fig. 2a). All of these transformations are reversible. The HTXRD pattern (Fig. 2b) helped to clarify these transformations. From ambient to 268°C it shows a mixture of monoclinic $BiVO_4$ and α-$Bi_4V_2O_{11}$. At 268°C the phase transition of monoclinic $BiVO_4$ to the tetragonal form occurs. This transition seems to be of second order since there is no thermal effect. The phase transformation of α-$Bi_4V_2O_{11}$ to the β form occurs at 455°C. At 575°C, γ-$Bi_4V_2O_{11}$ appears. No evidence of the existence of a $Bi_{6.67}O_4(PO_4)_4$-type phase was found, in agreement with the known phase diagram for the Bi_2O_3–V_2O_5 (7–9) binary system.

The DTA pattern of the composition $Bi_{6.67}As_4O_{20}$ does not display any other peak than the one corresponding to the melting point around 960°C (Fig. 3a). The HTXRD powder pattern from 500°C to 960°C is far more complicated (Fig. 3b). The literature concerning the binary system Bi_2O_3–As_2O_5 is rather incomplete. At ambient the mixture consists of rooseveltite, α-$BiAsO_4$, which is monoclinic, and $Bi_4As_2O_{11}$. HTXRD patterns of each of these compounds were obtained in order to explain the phenomena at high temperature. The first transformation occurs at 871°C and concerns α-$BiAsO_4$. At 883°C, 926°C, and 950°C, successive transformations of $Bi_4As_2O_{11}$ occur. Further experiments need to be performed to explain in detail these phenomena.

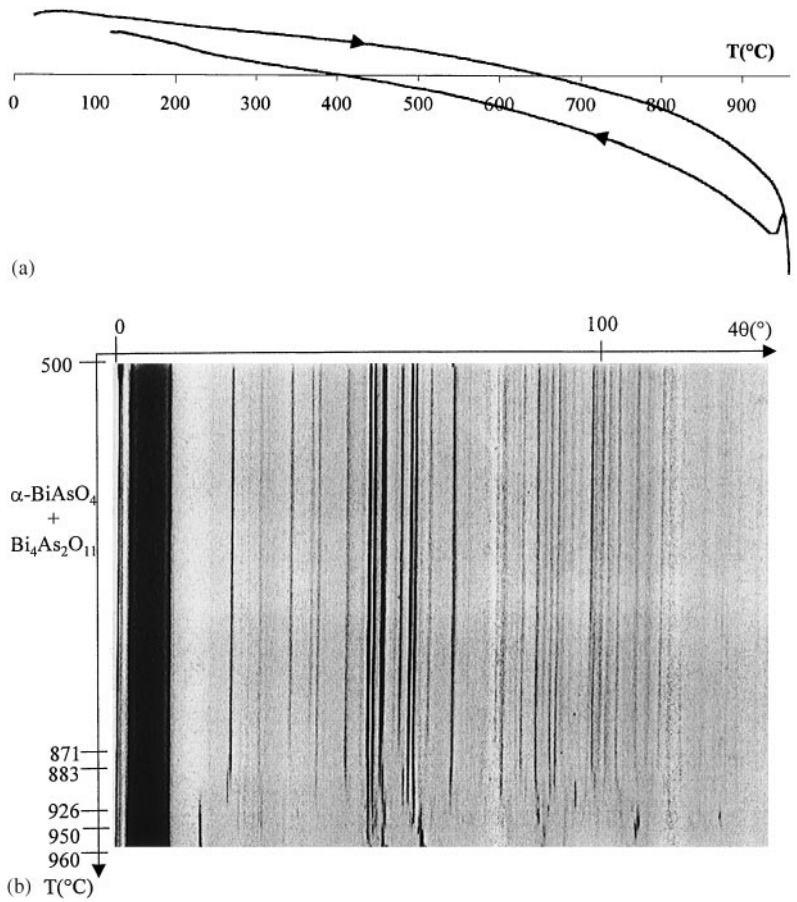

FIG. 3. Thermal analysis of the composition $Bi_{6.67}O_4(AsO_4)_4$. (a) DTA and (b) HTXRD.

TABLE 1
Powder Diffraction Patterns of (a) $PbBi_6O_4(PO_4)_4$, and (b) $PbBi_6O_4(VO_4)_4$, and (c) $PbBi_6O_4(AsO_4)_4$

h	k	l	d_{obs} (Å)	d_{calc} (Å)	I/I_O (%)	h	k	l	d_{obs} (Å)	d_{calc} (Å)	I/I_O (%)
				(a) $PbBi_6O_4(PO_4)_4$							
0	1	0	6.602	6.602	24	2	−2	2	2.624	2.623	11
1	−1	0	6.423	6.425	2	3	−2	1	2.618	2.616	3
0	0	1	6.362	6.362	10	1	−1	−2	2.597	2.597	4
0	1	−1	5.978	5.974	9	0	2	1	2.533	2.534	< 1
1	0	−1	5.674	5.675	6	2	1	1	2.508	2.508	3
1	−1	1	5.244	5.246	5	0	1	2	2.492	2.492	2
1	0	1	4.709	4.708	8	3	1	−1	2.473	2.473	5
1	1	0	4.554	4.545	< 1	3	0	1	2.452	2.453	2
2	0	0	4.326	4.324	10	2	−3	1	2.445	2.445	1
1	−1	−1	4.032	4.031	30	0	3	−1	2.409	2.409	16
2	0	−1	3.943	3.949	< 1	1	−3	2	2.365	2.366	3
0	1	1	3.852	3.855	2	2	0	2	2.354	2.354	2
2	−1	1	3.743	3.743	14	1	−3	0	2.334	2.334	< 1
1	−2	1	3.693	3.690	< 1	0	1	−3	2.316	2.316	< 1
0	2	−1	3.599	3.599	26	4	−1	0	2.303	2.303	5
1	−2	0	3.514	3.515	8	1	1	−3	2.290	2.290	2
0	1	−2	3.480	3.481	1	3	1	−2	2.254	2.253	6
0	2	0	3.301	3.301	11	1	2	1	2.235	2.234	13
2	0	1	3.293	3.292	25	3	−2	2	2.224	2.224	3
1	1	−2	3.264	3.263	100	1	−2	3	2.200	2.200	5
2	−2	1	3.220	3.221	61	3	−1	2	2.189	2.189	7
1	−1	2	3.195	3.197	6	1	−1	3		2.189	
1	1	1	3.168	3.166	3	1	2	−3	2.168	2.168	3
2	1	0	3.153	3.153	59	3	−3	0	2.142	2.142	16
3	−1	0	3.056	3.057	15	4	−1	1	2.124	2.124	11
1	−2	2	2.943	2.945	< 1	1	3	−2	2.117	2.117	3
3	0	0	2.882	2.883	1	2	0	−3	2.069	2.069	7
3	0	−1	2.841	2.840	7	3	−3	2	2.036	2.036	1
1	0	2	2.815	2.814	28	3	1	1	2.020	2.020	4
1	2	0	2.781	2.781	6	3	2	−1	2.003	2.004	2
3	−1	−1	2.770	2.771	39	1	−3	3	1.999	1.999	12
1	2	−2	2.716	2.716	4	4	0	−2	1.975	1.974	5
1	−2	−1	2.693	2.693	37	3	2	−2	1.952	1.951	12
3	−2	0	2.678	2.677	2						
				(b) $PbBi_6O_4(VO_4)_4$							
0	1	0	6.872	6.872	22	2	−3	1	2.529	2.528	2
1	−1	0	6.596	6.599	4	0	3	−1	2.521	2.521	19
0	0	1	6.478	6.475	15	3	0	1	2.490	2.490	3
0	1	−1	6.201	6.200	8	1	−3	2	2.457	2.457	3
1	0	−1	5.805	5.806	5	3	1	0	2.420	2.421	< 1
1	−1	1	5.346	5.353	4	0	3	−2	2.412	2.412	3
1	0	1	4.776	4.775	15	2	0	2	2.388	2.388	9
2	0	0	4.401	4.401	18	0	1	−3	2.365	2.365	2
1	−1	−1	4.127	4.126	32	1	1	−3	2.346	2.347	4
2	0	−1	4.042	4.039	1	4	−1	0	2.337	2.336	6
0	1	1	3.950	3.952	4	3	1	−2	2.322	2.322	7
2	−1	1	3.790	3.791	6	1	2	1	2.301	2.301	12
0	2	−1	3.765	3.766	13	3	−2	2	2.259	2.258	3
1	−2	0	3.643	3.643	8	1	−2	3	2.252	2.252	2
0	2	0	3.436	3.436	18	1	2	−3	2.240	2.241	4
1	1	−2	3.363	3.363	100	1	−1	3	2.225	2.226	10
2	0	1	3.340	3.340	46	1	3	−2	2.214	2.214	5
2	−2	0	3.299	3.299	63	3	−3	0	2.200	2.200	18
2	−2	1		3.300		0	0	3	2.158	2.158	3
2	1	0	3.244	3.244	85	4	−1	1	2.149	2.150	17
3	−1	0	3.101	3.101	21	4	−2	1		2.149	

TABLE 1—*Continued*

h	k	l	d_{obs} (Å)	d_{calc} (Å)	I/I_O (%)	h	k	l	d_{obs} (Å)	d_{calc} (Å)	I/I_O (%)
1	−2	2	3.029	3.030	2	2	0	−3	2.114	2.114	6
3	0	0	2.934	2.934	7	3	2	−1	2.076	2.076	2
2	0	−2	2.903	2.903	7	2	−2	−2	2.063	2.063	17
3	0	−1		2.902		1	−3	3		2.063	
1	2	0	2.888	2.889	10	3	2	−2	2.023	2.023	12
1	0	2	2.857	2.857	48	4	0	−2	2.020	2.020	5
3	−1	−1	2.822	2.822	61	1	0	3	2.005	2.005	6
1	−2	−1	2.772	2.772	52	2	−1	3	1.997	1.997	2
3	−1	1		2.772		2	1	2	1.973	1.973	6
3	−2	0	2.730	2.730	4	2	2	1		1.973	
2	−2	2	2.677	2.677	10	1	3	−3	1.964	1.965	3
2	−2	−1		2.677		4	−1	−2	1.961	1.961	1
3	−2	1	2.661	2.661	2	2	−3	3	1.955	1.955	7
1	−1	−2	2.652	2.652	12	2	−4	2	1.913	1.913	3
2	1	1	2.564	2.564	6	4	−2	2	1.896	1.895	6
3	1	−1	2.546	2.546	8	2	−1	−3	1.891	1.891	20
0	1	2	2.544	2.543	9						
				(c) $PbBi_6O_4(AsO_4)_4$							
1	1	0	6.806	6.811	15	1	−3	2	2.420	2.420	4
1	−1	0	6.579	6.584	1	1	−3	0	2.407	2.406	1
0	0	1	6.471	6.467	5	2	0	2	2.382	2.382	3
0	1	−1	6.107	6.107	4	0	3	−2	2.372	2.372	3
1	0	−1	5.811	5.809	3	0	1	−3	2.351	2.352	2
1	−1	1	5.307	5.305	3	4	−1	0	2.340	2.340	4
1	0	1	4.766	4.765	5	2	2	0	2.334	2.334	2
2	−1	0	4.455	4.453	2	3	1	−2	2.312	2.311	3
2	0	0	4.397	4.398	4	0	2	−3	2.297	2.297	2
1	−1	−1	4.138	4.137	10	1	2	1	2.291	2.292	7
0	1	1	3.947	3.949	1	3	−2	2	2.245	2.246	4
2	−1	1	3.775	3.777	6	1	−2	3	2.229	2.229	2
1	−2	1		3.776		4	−2	0	2.226	2.227	1
0	2	−1	3.703	3.705	9	1	3	−1		2.225	
1	−2	0	3.620	3.620	8	1	−1	3	2.214	2.214	8
0	2	0	3.406	3.405	17	3	−1	2	2.207	2.208	2
1	1	−2	3.336	3.337	100	4	0	0	2.200	2.199	2
2	0	1	3.331	3.333	15	3	−3	0	2.195	2.195	10
2	−2	0	3.292	3.292	6	1	3	−2	2.180	2.180	3
2	−2	1	3.274	3.274	69	0	0	3	2.157	2.156	1
2	1	0	3.226	3.226	63	4	−1	1	2.147	2.148	15
3	−1	0	3.105	3.106	11	2	0	−3	2.114	2.114	3
1	−2	2	2.992	2.991	1	3	1	1	2.057	2.057	3
3	0	0	2.933	2.932	2	2	−2	3	2.046	2.046	< 1
2	0	−2	2.905	2.905	4	1	−3	3	2.034	2.034	15
3	0	−1		2.904		4	0	−2	2.021	2.021	3
1	2	0	2.864	2.863	6	1	−3	−1	2.017	2.019	1
1	0	2	2.852	2.851	31	3	2	−2	2.004	2.005	13
3	−1	−1	2.833	2.833	51	1	0	3	2.001	2.001	4
1	2	−2	2.788	2.789	4	4	1	−1	1.997	1.998	3
1	−2	−1	2.771	2.770	40	2	−1	3	1.989	1.988	2
3	−2	0	2.732	2.731	3	4	−1	−2	1.969	1.969	2
1	−1	−2	2.658	2.657	4	2	2	1	1.964	1.964	3
2	−2	2	2.653	2.653	11	4	−3	1	1.960	1.959	1
2	1	1	2.556	2.556	3	1	3	−3	1.936	1.936	1
0	1	2	2.544	2.544	3	2	−3	3	1.933	1.933	6
3	1	−1	2.534	2.534	8	1	−4	1	1.929	1.929	3
2	−3	1	2.503	2.503	1	2	−1	−3	1.895	1.895	14
0	3	−1	2.485	2.485	22	4	−2	2	1.889	1.889	6

TABLE 2
Cell Parameters for $PbBi_6O_4(PO_4)_4$, $PbBi_6O_4(AsO_4)_4$, and $PbBi_6O_4(VO_4)_4$ Used to Index the Powder Patterns and Indexes of Merit

Compound	a (Å)	b (Å)	c (Å)	α (°)	β (°)	γ (°)	V (Å^3)
$Bi_{6.67}O_4(PO_4)_4$	9.195(15)	7.552(5)	6.933(4)	112.2(1)	93.9(1)	106.9(1)	418(1)
$PbBi_6O_4(PO_4)_4$[a]	9.231(2)	7.589(1)	6.996(1)	112.038(9)	93.429(9)	107.274(9)	426.6(2)
$PbBi_6O_4(AsO_4)_4$[b]	9.387(1)	7.803(1)	7.113(1)	111.746(7)	94.316(7)	106.791(2)	454.2(2)
$PbBi_6O_4(VO_4)_4$[c]	9.369(1)	7.906(1)	7.163(1)	112.638(5)	94.023(5)	106.411(5)	460.8(2)

Note. All powder patterns were obtained with Cu$K\alpha$ radiation.
[a] $F(30) = 78.1(0.0094; 41)$, $M(20) = 38.9(3.2523; 25)$.
[b] $F(30) = 84.7(0.0075; 47)$, $M(20) = 43.4(3.2146; 32)$.
[c] $F(29) = 131.5(0.0044; 50)$, $M(20) = 65.7(3.0905; 35)$.

However, no arsenate corresponding to the phase $Bi_{6.67}O_4(PO_4)_4$ was observed under these experimental conditions.

The compounds $PbBi_6O_4(XO_4)_4$ (X = P (1), V, and As) exist at room temperature. The powder diffraction patterns are shown in Tables 1a, 1b, and 1c. Cell parameters are reported in Table 2. The volume of the cell increases when one Pb, leading to the compound $PbBi_6O_4(PO_4)_4$, replaces two-thirds of the Bi in $Bi_{6.67}O_4(PO_4)_4$ Thereafter the cell volume increases regularly from the phosphate to the arsenate, and from the arsenate to the vanadate according to the cationic tetrahedral radii $r(P^{5+}) = 0.17$ Å, $r(As^{5+}) = 0.335$ Å, and $r(V^{5+}) = 0.353$ Å, (23). The refinement of the structure of $PbBi_6O_4(PO_4)_4$ was performed on polycrystalline material using the Rietveld profile method by means of the program FULLPROF (22). The previously refined cell parameters were introduced into the program. The intensities were extracted from the powder patterns using a cell-constrained, whole pattern fitting program. Initially no reference to a structural model is needed. After-

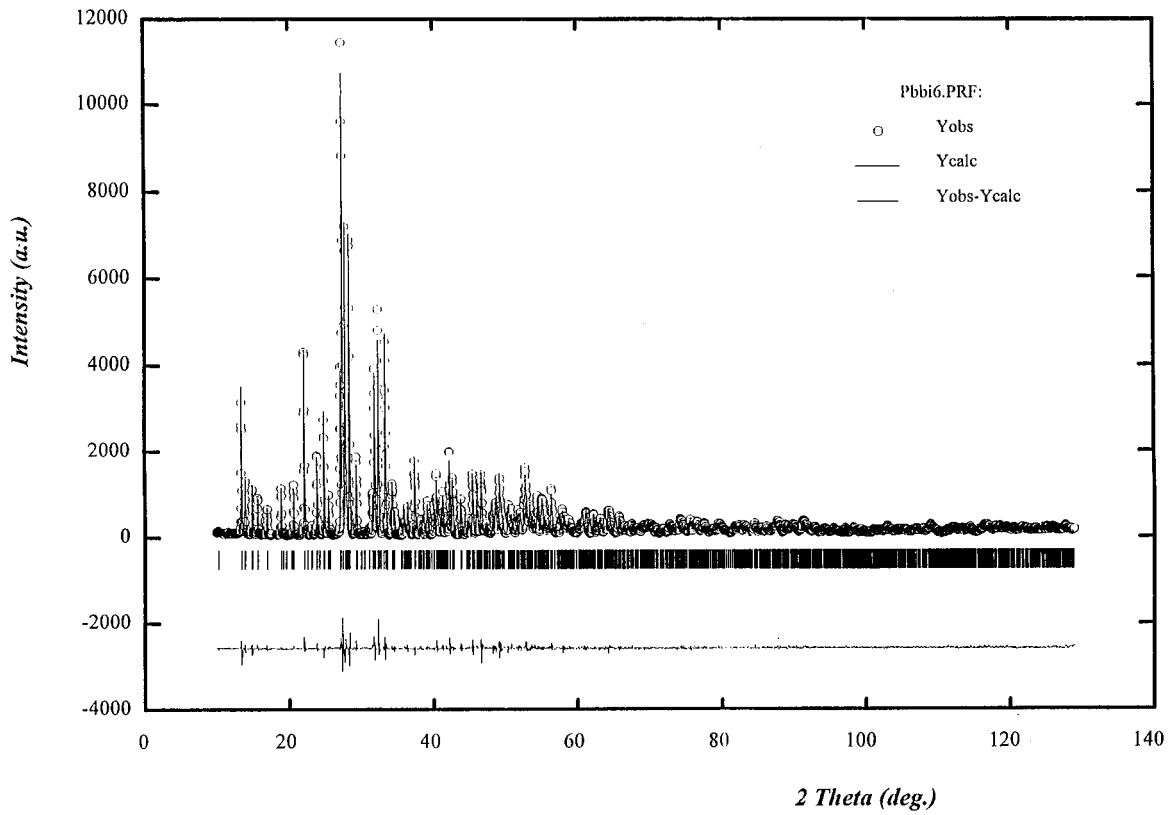

FIG. 4. Rietveld refinement of the X-ray diffraction powder pattern of $PbBi_6O_4(PO_4)_4$.

TABLE 3
Rietveld Parameters and Refinement for $PbBi_6O_4(PO_4)_4$

Space group	$P\bar{1}$
Cell parameters, Å, deg	
a	9.2309(3)
b	7.5875(2)
c	6.9978(2)
α	111.978(2)
β	93.436(2)
γ	107.291(2)
Volume, Å^3	425.78(3)
Z	1
2θ range, deg	10–129
Step scan, 2θ, deg	0.03
Time/step, s	54
Number of reflections	2855
Number of refined parameters	92
Zero point, 2θ, deg	0.0867(9)
Profile function	Pseudo-Voigt, $\eta = 0.38(2)$
Profile parameters	
U	0.090(4)
V	−0.040(3)
W	0.0125(5)
$R_{wp} = \left[\sum_i w_i (y_i - y_{ci})^2 \Big/ \sum_i w_i y_i^2\right]^{1/2}$	11.7%
$R_p = \sum_i \lvert y_i - y_{ci}\rvert / \sum_i y_i$	9.40%
$R_F = \sum \lvert\lvert F_{\text{"obs"}}\rvert - \lvert F_{calc}\rvert\rvert / \sum \lvert F_{\text{"obs"}}\rvert$	2.26%
$R_{Bragg} = \sum_k / I_k - I_k^{calc} / / \sum_k I_k$	3.73%
χ^2	2.63

ward the atomic positions of $Bi_{6.67}O_4(PO_4)_4$ (1) were used as a starting model in the refinements. The peak shape was represented by a pseudo-Voigt function with an asymmetry correction at low angles. The background was refined by a polynomial in 2θ. The dependence between the full width at half-maximum, H, and the angle was represented by $H^2 = U \operatorname{tg} 2\theta + V \operatorname{tg} \theta + W$, where U, V, and W were refined. The procedure involved the refinement of the 2θ zero

TABLE 4
Atomic Positions and Isotropic or Equivalent Thermal Displacement Parameters for $PbBi_6O_4(PO_4)_4$

Atom	x	y	z	$B_{eq}{}^a / B$ (Å^2)
Bi(1)	0.3274(3)	0.3065(4)	0.8063(5)	0.49(3)[a]
Bi(2)	0.0848(4)	0.7830(5)	0.4342(5)	1.12(3)[a]
Bi(3)	0.5080(3)	0.1268(4)	0.3331(4)	0.65(3)[a]
Pb	0	0	0	1.84(3)[a]
P(1)	0.759(2)	0.273(3)	0.057(3)	1.1(4)[a]
P(2)	0.743(2)	0.601(3)	0.652(3)	0.6(4)[a]
O(1)	0.853(3)	0.167(5)	−0.124(5)	0.3(2)
O(2)	0.716(3)	0.729(5)	0.865(5)	0.3(2)
O(3)	0.766(3)	0.193(4)	0.211(5)	0.3(2)
O(4)	0.905(3)	0.894(5)	0.303(5)	0.3(2)
O(5)	0.688(3)	0.389(5)	0.636(5)	0.3(2)
O(6)	0.924(3)	0.665(5)	0.651(5)	0.3(2)
O(7)	0.636(3)	0.973(5)	0.434(5)	0.3(2)
O(8)	0.648(3)	0.601(5)	0.466(5)	0.3(2)
O(9)	0.604(4)	0.219(5)	−0.045(5)	0.3(2)
O(10)	0.835(4)	0.509(5)	0.138(5)	0.3(2)

[a] $B_{eq} = \frac{4}{3} \sum_i \sum_j \beta_{ij} a_i a_j$.

TABLE 5
Anisotropic Thermal Displacements, $\times 10^4$

Atom	β_{11}	β_{22}	β_{33}	β_{12}	β_{13}	β_{23}
Bi(1)	14(5)	13(10)	21(10)	1(6)	2(7)	−19(8)
Bi(2)	46(6)	76(11)	58(10)	36(6)	28(7)	26(8)
Bi(3)	7(6)	87(12)	10(10)	17(7)	1(7)	13(9)
Pb	52(9)	41(16)	130(17)	−1(9)	−72(9)	−1(13)

TABLE 6
Interatomic Distances (Å), Angles (°), and Valences (s)

	d	s		d	s
$Bi(1)–O(2)^{i}_{1\,1\,2}$	2.46(5)	0.37	$Bi(2)–O(1)^{i}_{1\,1\,0}$	2.41(5)	0.43
$Bi(1)–O(4)^{i}_{1\,1\,1}$	2.12(3)	0.93	$Bi(2)–O(3)^{i}_{1\,1\,1}$	2.68(4)	0.21
$Bi(1)–O(7)^{i}_{1\,1\,1}$	2.29(4)	0.59	$Bi(2)–O(4)_{\bar{1}00}$	2.35(4)	0.50
$Bi(1)–O(8)^{i}_{1\,1\,1}$	2.27(4)	0.62	$Bi(2)–O(4)^{i}_{1\,2\,1}$	2.42(3)	0.41
$Bi(1)–O(9)_{0\,0\,1}$	3.04(4)	0.08	$Bi(2)–O(5)^{i}_{1\,1\,1}$	2.76(4)	0.17
$Bi(1)–O(9)^{i}_{1\,1\,1}$	3.19(3)	0.05	$Bi(2)–O(6)_{\bar{1}00}$	2.41(4)	0.43
$Bi(1)–O(10)^{i}_{1\,1\,1}$	2.30(5)	0.57	$Bi(2)–O(6)^{i}_{1\,1\,1}$	3.20(4)	0.05
		3.21	$Bi(2)–O(7)^{i}_{1\,2\,1}$	2.55(3)	0.29
			$Bi(2)–O(10)_{\bar{1}00}$	2.70(3)	0.19
					2.68
$Bi(3)–O(1)^{i}_{1\,0\,0}$	3.28(3)	0.04	$Pb–O(1)_{\bar{1}00}$	2.43(5)	0.42
$Bi(3)–O(2)^{i}_{1\,1\,1}$	3.09(5)	0.07	$Pb–O(1)^{i}_{100}$	2.43(5)	0.42
Bi(3)–O(3)	2.55(4)	0.29	$Pb–O(2)_{\bar{1}\,\bar{1}\,\bar{1}}$	2.65(3)	0.23
Bi(3)–O(5)	2.38(3)	0.46	$Pb–O(2)^{i}_{111}$	2.65(3)	0.23
$Bi(3)–O(7)_{0\bar{1}0}$	2.14(5)	0.88	$Pb–O(3)_{-100}$	3.10(4)	0.07
$Bi(3)–O(7)^{i}_{1\,1\,1}$	2.35(4)	0.49	$Pb–O(3)^{i}_{\bar{1}00}$	3.10(4)	0.07
Bi(3)–O(8)	3.17(4)	0.05	$Pb–O(4)_{\bar{1}\bar{1}0}$	2.64(4)	0.24
$Bi(3)–O(8)^{i}_{1\,1\,1}$	2.86(4)	0.13	$Pb–O(4)_{110}$	2.64(4)	0.24
Bi(3)–O(9)	3.09(4)	0.07	$Pb–O(6)_{\bar{1}\bar{1}\bar{1}}$	2.65(4)	0.23
$Bi(3)–O(9)^{i}_{1\,0\,0}$	2.49(3)	0.34	$Pb–O(6)_{111}$	2.65(4)	0.23
		2.82			2.38
P(1)–O(1)	1.67(4)	0.87	P(2)–O(2)	1.53(4)	1.27
P(1)–O(3)	1.43(5)	1.66	P(2)–O(5)	1.49(5)	1.41
P(1)–O(9)	1.43(4)	1.66	P(2)–O(6)	1.60(4)	1.05
P(1)–O(10)	1.57(5)	1.14	P(2)–O(8)	1.53(5)	1.27
		5.33			5.00
	Angle			Angle	
O(1)–P(1)–O(3)	106(5)		O(2)–P(2)–O(5)	105(4)	
O(1)–P(1)–O(9)	108(5)		O(2)–P(2)–O(6)	110(5)	
O(1)–P(1)–O(10)	108(4)		O(2)–P(2)–O(8)	114(5)	
O(3)–P(1)–O(9)	112(5)		O(5)–P(2)–O(6)	108(4)	
O(3)–P(1)–O(10)	116(6)		O(5)–P(2)–O(8)	107(5)	
O(9)–P(1)–O(10)	107(4)		O(6)–P(2)–O(8)	113(5)	

Note. Symmetry transformation: i, $-x$, $-y$, $-z$; $O(1)^{i}_{1\,1\,0}$, $1-x$, $1-y$, $-z$.

TABLE 7
Electron Lone-Pair Positions for $PbBi_6O_4(PO_4)_4$

Atom X	x	y	z	$d(X-6s^2)$(Å)
Bi(1)	0.3761	0.2954	0.8246	0.4988
Bi(2)	0.1013	0.7640	0.4392	0.2474
Bi(3)	0.4709	0.1772	0.3004	0.6704
Pb	0	0	0	0.0000

displacement of the instrument, scale factor, cell parameters, atomic coordinates, and thermal parameters.

Isotropic displacement parameters were refined for the oxygen and phosphorus atoms and anisotropic parameters for the lead and bismuth atoms. The isotropic displacement parameters for oxygens were set to the same value. At the end of the refinement, the agreement between observed and calculated data was indicated by the reliability factors and by the plot of the observed and calculated patterns (Fig. 4). Final results of the Rietveld refinement are summarized in Table 3. The relatively high value of R_{wp} is typically observed for X-ray diffraction data. The atomic parameters, displacement parameters, interatomic distances, and bond valences (24) are reported in Tables 4, 5, 6.

The electron lone-pairs of the bismuth and lead atoms were localized using the theory of Verbaere *et al.* (25) incorporated in the computer program HYBRIDE (26). The lone-pair positions and their distances from Bi and Pb are shown in Table 7.

DISCUSSION

In $PbBi_6O_4(PO_4)_4$, the lead atom occupies the 1*a* site of space group $P\bar{1}$. In $Bi_{6.67}O_4(PO_4)_4$, the Bi occupies the same site with occupancy of 2/3. Otherwise, there are only slight differences in the atomic positions.

Bi(1) is bonded to five oxygen atoms, O(2), O(4), O(7), O(8), and O(10), at bond distances from 2.12(3) Å to 2.46(5) Å and two O(9) at distances > 3 Å, Fig. 7. These five oxygen ions form a distorted trigonal prism around Bi(1) in which the sixth atom is missing (13). The inclusion of the two long O(9) oxygen bonds results in the formation of a monocapped trigonal prism where O(9) at 3.04 Å is the capping atom. The repulsion by the lone-pair electrons causes the lengthening of the Bi(1)–O(9) bonds.

Bi(2) is surrounded by eight oxygen atoms at distances < 3 Å forming a somewhat distorted square antiprism, Fig. 5. The oxygen environment is relatively symmetric and explains the short distance between bismuth and the lone-pair.

Bi(3) is surrounded by six oxygen atoms, O(3), O(5), two O(7), O(8), and O(9), at distances < 3 Å, Fig. 5. The coordination polyhedron is similar to that of Bi(1). The lone-pair repulsion is responsible for some of the oxygens at bond lengths > 3 Å.

The coordination polyhedron around Pb consists of eight atoms, two O(1), two O(2), two O(4), and two O(6) at < 3 Å, that form a slightly distorted cube, Fig. 5. The high symmetry of the oxygen environment does not permit the hybridization of the lone pair and it has *s*-orbital character centered on the Pb nucleus. The phosphate groups form tetrahedra with bond lengths and angles that can be considered the same within 3σ and correspond to values usually observed for PO_4 groups.

Bond valences sums, shown in Table 6, are 5.33 and 5 for the phosphorus atoms as expected. The values of Bi(1), Bi(2), and Bi(3) are respectively 3.21, 2.68, and 2.82. The value for Bi(2) is quite low compared to the expected value of 3. It is compensated by the relatively high value of the bond valence sum for Pb, 2.38. It could be due to the existence of mixed site Bi/Pb occupancy that cannot be resolved by X-ray diffraction.

Figure 6 displays the bismuth and lead atoms and the oxygen environment linking these atoms in the *ac* plane. Chains of $(Bi_6O_4)_\infty$ parallel to *a* are present and they are linked by O(4)–Pb–O(4) bridges. A description based on polyhedra where an oxygen atom is surrounded by a tetragonal arrangement of heavy atoms is possible. Two central tetrahedra, O–Bi_4, link by sharing a Bi–Bi edge. This binuclear unit is terminated at each end by O–$PbBi_3$ tetrahedra

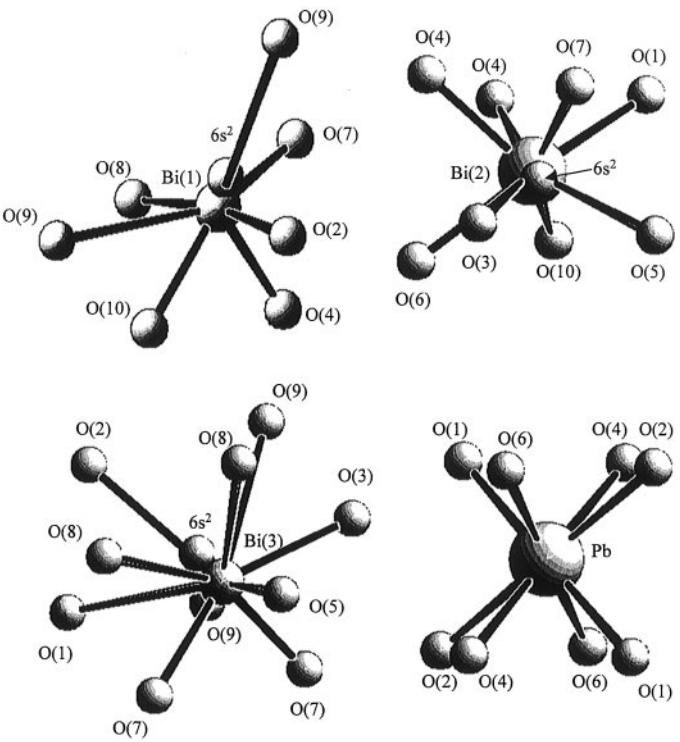

FIG. 5. Oxygen environments of bismuth and lead atoms in $PbBi_6O_4(PO_4)_4$.

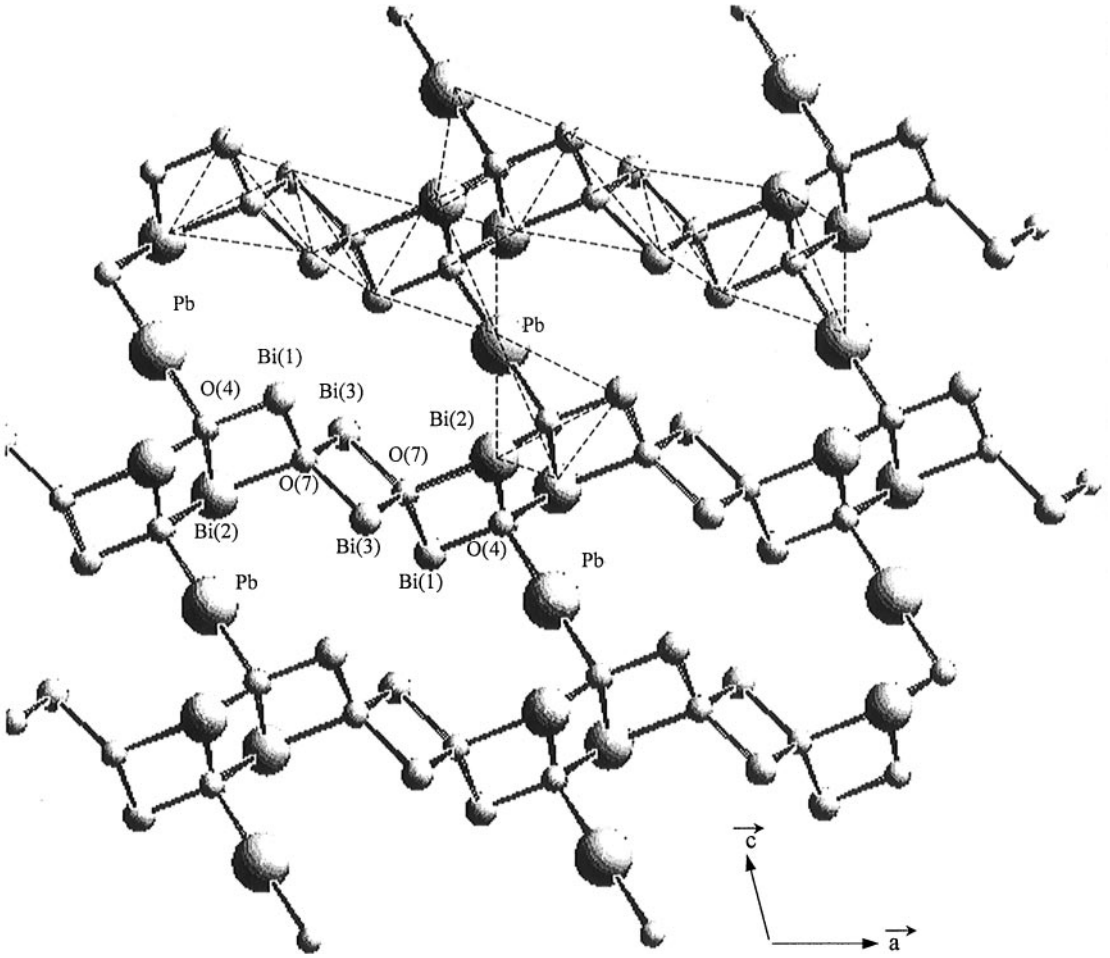

FIG. 6. $(Bi_6O_4)_\infty$ chains in the a–c plane.

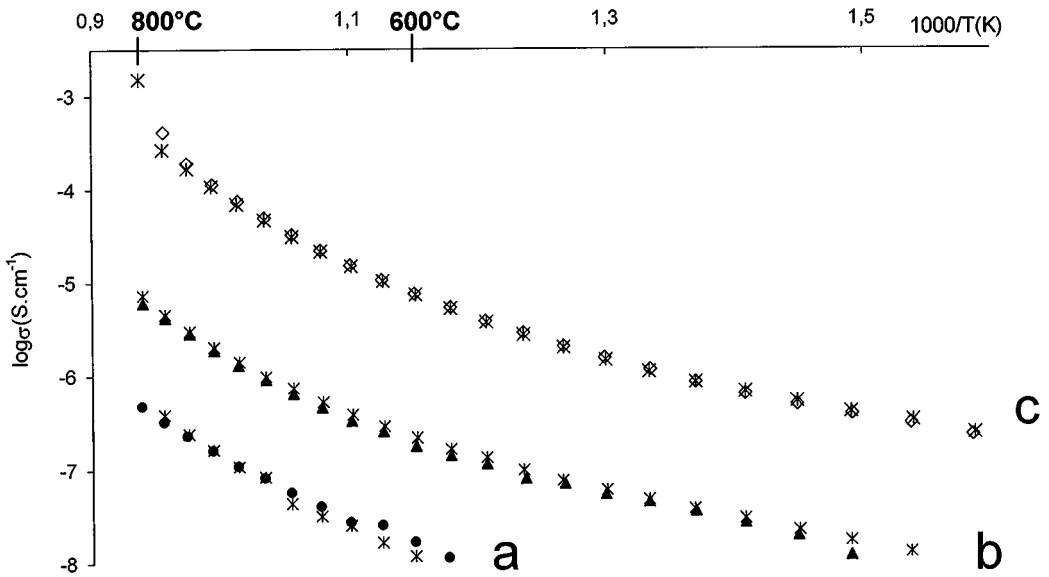

FIG. 7. Arrhenius plots of log σ vs $1000/T$. Heating and cooling curves for (a) $PbBi_6O_4(PO_4)_4$; (b) $PbBi_6O_4(AsO_4)_4$; (c) $PbBi_6O_4(VO_4)_4$.

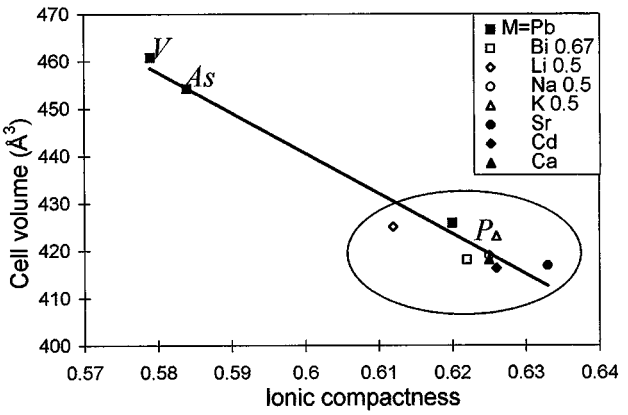

FIG. 8. Evolution of the unit cell volume versus the ratio ion volume/cell volume for the $MBiO_4(XO_4)_4$ series.

that are shared by the next binuclear units to lead to infinite chains parallel to the *a* axis. These chains are linked into layers by the sharing of the apical Pb of the $O–PbBi_3$ tetrahedra. The layers are spanned by the XO_4 tetrahedra into a three-dimensional structure.

The conductivity measurements, $\log\sigma$ vs $1000/T$, are shown (Figs. 7a, b, c) for the heating and cooling cycles. Good reproducibility of the conductivity measurements is observed in agreement with the absence of any phase transition in the corresponding temperature range. When $X = P$, the low conductivity level does not allow accurate impedance measurements below 550°C. Above this temperature, σ increases progressively and reaches 5×10^{-7} S. cm^{-1} at 800°C, with 1.51 eV for the corresponding energy of activation. When $X =$ As the conductivity at that same temperature is 6.3×10^{-6} $S.cm^{-1}$. The conductivity for the sample with $X =$ V shows an increase to 4×10^{-3} $S.cm^{-1}$ at 800°C, very close to the melting point. As shown in other compounds in the $Bi_2O_3–PbO–X_2O_5$ systems (27) with $X =$ P, V, or As, the vanadates always have the highest conductivity. This may be interpreted in terms of ionic packing in the related structures of the $MBiO_4(XO_4)_4$ family (1, 27). We observe a linear evolution of the unit cell volume versus the ratio ionic volume/cell volume, Fig. 8. $PbBi_6O_4(VO_4)_4$ exhibits the lowest such ratio for the highest cell volume, thus facilitating the ionic migration through the structure.

CONCLUSION

The phase $PbBi_6O_4(XO_4)_4$, ($X =$ P, V, and As) exist at room temperature. They are isomorphs of the high-temperature compound $Bi_{6.67}O_4(PO_4)_4$ in which Pb replaces 0.67 Bi in a distinct crystallographic site. The binary vanadate and arsenate phases corresponding to the $Bi_{6.67}O_4(PO_4)_4$ phase do not exist under the same synthetic conditions. $PbBi_6O_4(VO_4)_4$ has the highest conductivity at 800°C, 4×10^{-3} $S.cm^{-1}$, of the homologous series.

ACKNOWLEDGMENTS

H.S. gratefully acknowledges the support of the R. A. Welch Foundation, Houston, Texas.

REFERENCES

1. M. Ketatni, O. Mentre, F. Abraham, F. Kzaiber, and B. Mernari, *J. Solid State Chem.* **139,** 254 (1998).
2. V. V. Volkov, L. A. Zhereb, Y. F. Kargin, V. M. Skorikov, and I. V. Tananaev, *Russ. J. Inorg. Chem.* **28**(4), 568 (1983).
3. J. P. Wignacourt, M. Drache, P. Conflant, and J. C. Boivin, *J. Chim. Phys.* **88,** 1933 (1991).
4. A. Watanabe, *Solid State Ionics* **96,** 55 (1995).
5. N. N. Chudinova, A. V. Lavrov, and I. V. Tananaev, *Izv. Akad. Nauk SSSR, Ser. Neorg. Mater.* **11,** 1951 (1952).
6. K. Palkina and K. H. Jost, *Acta Crystallogr. B* **31,** 2281 (1955).
7. Y. A. Blinovskov and A. A. Fotiev, *Russ. J. Inorg. Chem.* **32**(1), 145 (1987).
8. M. Touboul and C. Vachon, *Thermochim. Acta* **133,** 61 (1988).
9. M. F. Debreuille-Gresse, Thèse de doctorat, U. S. T. Lille, 1986.
10. N. M. Sammes, G. A. Tompsett, H. Nafe, and F. Aldinger, *J. Eur. Ceram. Soc.* **19,** 1801 (1999).
11. J. C. Boivin and G. Mairesse, *Chem. Mater.* **10,** 2850 (1998).
12. Y. C. Jie and W. Eysel, *Powder Diffraction* **10**(2), 56 (1995).
13. A. Mizrahi, J. P. Wignacourt, and H. Steinfink, *J. Solid State Chem.* **133,** 516 (1997).
14. A. Mizrahi, J. P. Wignacourt, M. Drache, and P. Conflant, *J. Mater. Chem.* **5**(6), 901 (1995).
15. L. H. Brixner and C. M. Foris, *Mater. Res. Bull.* **9,** 253 (1974).
16. M. Ketatni, Thèse de doctorat, U. S. T. Lille, 1995.
17. F. Abraham, M. Ketatni, G. Mairesse, and B. Mernari, *Eur. J. Solid State Inorg. Chem.* **31,** 313 (1994).
18. J. Huang and A. W. Sleight, *J. Solid State Chem.* **100,** 150 (1992).
19. J. Huang, Q. Gu, and A. W. Sleight, *J. Solid State Chem.* **105,** 599 (1993).
20. S. Giraud, J. P. Wignacourt, M. Drache, G. Nowogrocki, and H. Steinfink, *J. Solid State Chem.* **142,** 80 (1999).
21. S. Giraud, P. Conflant, M. Drache, J. P. Wignacourt, and H. Steinfink, *Phosphorus Res. Bull.* **10,** 138 (1999).
22. J. Rodriguez-Carvajal, M. T. Fernandez-Diaz, and J. L. Martinez, *J. Phys. Condens. Matter* **3,** 3215 (1991).
23. R. D. Shannon and C. T. Prewitt, *Acta Crystallogr. B* **25,** 925 (1969).
24. I. D. Brown and D. Altermatt, *Acta Crystallogr. B* **41,** 244 (1985).
25. A. Verbaere, R. Marchand, and M. Tournoux, *J. Solid State Chem.* **23,** 383 (1978).
26. E. Morin, G. Wallez, S. Jaulmes, J. C. Couturier, and M. Quarton, *J. Solid State Chem.* **137,** 283 (1998).
27. S. Giraud, Thèse de Doctorat, U. S. T. Lille, 1999.